AGU PUBLICATIONS

Geophysical Research Letters

RESEARCH LETTER
10.1002/2013GL059055

Key Points:
- First austral summer evaluation of land-atmosphere coupling strength
- Australia is a summer soil moisture-atmosphere coupling hot spot region
- TMAX coupling most sensitive to soil moisture and then atmospheric model physics

Supporting Information:
- Readme
- Table S1 and Figures S1–S7

Correspondence to:
A. L. Hirsch,
a.hirsch@student.unsw.edu.au

Citation:
Hirsch, A. L., A. J. Pitman, S. I. Seneviratne, J. P. Evans, and V. Haverd (2014), Summertime maximum and minimum temperature coupling asymmetry over Australia determined using WRF, *Geophys. Res. Lett.*, *41*, 1546–1552, doi:10.1002/2013GL059055.

Received 16 DEC 2013
Accepted 7 FEB 2014
Accepted article online 11 FEB 2014
Published online 5 MAR 2014

Summertime maximum and minimum temperature coupling asymmetry over Australia determined using WRF

A. L. Hirsch[1], A. J. Pitman[1], S. I. Seneviratne[2], J. P. Evans[1], and V. Haverd[3]

[1]ARC Centre of Excellence for Climate System Science and Climate Change Research Centre, University of New South Wales, Sydney, New South Wales, Australia, [2]Institute for Atmospheric and Climate Science, ETH Zurich, Zurich, Switzerland, [3]CSIRO Marine and Atmospheric Research, Canberra, ACT, Australia

Abstract Using the Weather and Research Forecasting model we derive the first estimates for intraseasonal soil moisture-atmosphere coupling strength for the Australian summer climate using methodology adapted from the Global Land-Atmosphere Coupling Experiment. We examine the variations in coupling strength by perturbing the background climate (dry versus wet year) and the model physics (planetary boundary layer or cumulus scheme). For all choices of model physics, results identify Australia as a "hot spot" of soil moisture-atmosphere coupling for both mean and maximum temperatures. For the wet case, results are consistent for maximum temperature for all physics choices. Results diverge more for maximum temperature in the chosen dry year. The coupling of soil moisture with minimum temperature is weaker but consistent for all choices of model physics or whether a wet or dry year is used. Coupling strength for precipitation is weak and not statistically significant irrespective of the choice of model physics.

1. Introduction

The Global Land Atmosphere Coupling Experiment (GLACE) [*Koster et al.*, 2004, 2006] evaluated land-atmosphere coupling over boreal summer (June-July-August) using a range of Atmospheric General Circulation Models. The widely used GLACE-1 coupling strength is a measure of the atmospheric sensitivity to variations in the land surface state, most commonly via soil moisture variability. While *Koster et al.* [2004, 2006] identified regions of strong coupling using a multimodel consensus there was a wide range of coupling strengths reported from the models. The parameterization differences between participating models limited the diagnosis of why some models were more strongly coupled than others [*Koster et al.*, 2006; *Guo et al.*, 2006].

Koster et al. [2006] did not identify Australia as a potential "hot spot" of land-atmosphere coupling. This was likely due to the focus of GLACE-1 and indeed GLACE-2 [*Koster et al.*, 2010] on the boreal summer. The mechanisms that strongly couple the land with the atmosphere tend to be most clear when net radiation is reasonably high and soil moisture limits evaporation. This is more likely the case in the respective regions' dry seasons. *Koster et al.* [2006] focus on boreal summer limited the conclusions that could be reached for the Southern Hemisphere. In contrast, a recent global-scale observation-based analysis relating temperature extremes in each region's hottest month with preceding precipitation deficits did highlight Australia and some other Southern Hemisphere midlatitude regions as potential "hot spots" of coupling between soil moisture and extreme temperatures [e.g., *Mueller and Seneviratne*, 2012].

In this study, we diagnose soil moisture-atmosphere coupling strength by adapting the GLACE-1 methodology for implementation in the Weather Research and Forecasting (WRF) regional climate model [*Skamarock et al.*, 2008] over Australia. Focusing on the austral summer (DJF, December-January-February), we examine four different combinations of WRF parameterizations using two alternative planetary boundary layer (PBL) schemes and two alternative cumulus convection schemes. Each combination is run in an El Niño-like (dry) and La Niña-like (wet) state to bracket the coupling sensitivity to interannual soil moisture variability.

We note that the sensitivity of coupling strength to model physics has been examined previously. *Wei and Dirmeyer* [2010] used two different atmospheric models and three different land surface models (LSMs). They showed that the atmospheric models had a greater impact on the spatial distribution and amplitude of precipitation variability and land-atmosphere coupling strength, while the impact of the LSM on the

coupling was mostly limited to regional scales. *Guo and Dirmeyer* [2013] extended the GLACE-1 methodology to consider the interannual variability of land-atmosphere coupling strength in one model. They identified significant year-to-year variations in coupling strength associated with soil moisture anomalies over the transitional regions identified in *Koster et al.* [2006]. Finally, *Mei et al.* [2013] used the GLACE-1 methodology in a regional domain for the U.S. to show that soil moisture-temperature coupling strength estimates were broadly consistent with *Koster et al.* [2006].

Our paper is the first to examine the sensitivity of coupling strength to model physics over Australia. It is also the first to examine the coupling strength for maximum and minimum temperatures separately. This is significant since soil moisture anomalies would be expected to affect maximum and minimum temperatures differently [*Jaeger and Seneviratne*, 2011]. Strong variations in coupling strength linked with physics, and significant differences between coupling strength for maximum as distinct from minimum temperatures, would raise questions around how to parameterize processes linked to the land's role in simulating extremes.

2. Model Description and Experimental Design

2.1. Model Description

We use WRF coupled to the Community Atmosphere Biosphere Land Exchange (CABLE) model [*Wang et al.*, 2011] using the NASA Land Information System (LIS) [*Kumar et al.*, 2006] as described in *Hirsch et al.* [2014]. The model domain is centered at 24.26°S and 147.63°E with a spatial resolution of 50 km, 30 atmospheric levels, 6 soil layers, and a model time step of 180 seconds. Lateral boundary conditions use ERA-Interim reanalysis data [*Dee et al.*, 2011].

We implement two PBL schemes: Yonsei University (YSU) and Mellor-Yamada-Janjic (MYJ). These differ in closure order, the representation of vertical mixing and require different surface layer schemes. Note that YSU is technically a local scheme that has a counter-gradient term to represent nonlocal fluxes. We implement two cumulus schemes: the mass flux scheme of Kain-Fritsch (KF) and the adjustment cumulus scheme of Betts-Miller-Janjic (BMJ). Only the PBL and cumulus schemes are varied as they have the greatest impact on the WRF simulations for this domain [*Evans et al.*, 2012]. Other components of WRF are identical and are listed in Table S1 in the supporting information.

2.2. Experimental Design

Our GLACE-like experiments follow *Koster et al.* [2006] and are performed for each of the four different physics configurations with all simulations corresponding to austral summer (DJF). Each experiment consists of a coupled and uncoupled 16-member ensemble. The coupled ensemble consists of simulations with two-way interaction between the land and atmosphere enabled. From one coupled ensemble simulation, the subsurface soil moisture is saved at every model time step. These are then read back into the model for the uncoupled experiments to prescribe the subsurface soil moisture at every model time step. This effectively decouples the land-atmosphere feedback.

Koster et al. [2006] suggest five methods for initializing the ensemble members: one uses the initial date (here 1 December) values from various years from a single simulation. Our simulations are forced by ERA-interim lateral boundary conditions, so an analogous approach is implemented where different 1 December values from different reanalysis years are used for the initial atmospheric conditions. The land surface initial conditions were obtained from 4 year offline CABLE simulations for each ensemble member to obtain equilibrated land surface states (e.g., soil moisture) that were internally consistent with CABLE. By using different years for the boundary conditions the simulations capture interannual variability across the region.

GLACE-1 examined a neutral El Niño Southern Oscillation (ENSO) year. ENSO is a dominant mode of variability in Australia [*Risbey et al.*, 2009] and has a profound impact on interannual variability. Therefore, we modified the GLACE-1 setup to consider the impact of the background climate for resulting measures of soil moisture-atmosphere coupling. For each physics configuration we used one summer corresponding to dry (El Niño: December 1982 to February 1983) and one corresponding to wet (La Niña: December 1999 to February 2000) soil moisture conditions. The dry (wet) summer soil moisture case was selected from all available years as that with the highest percentage of grid cells where the soil moisture and precipitation anomalies were one standard deviation below (above) the climatological mean for both DJF and

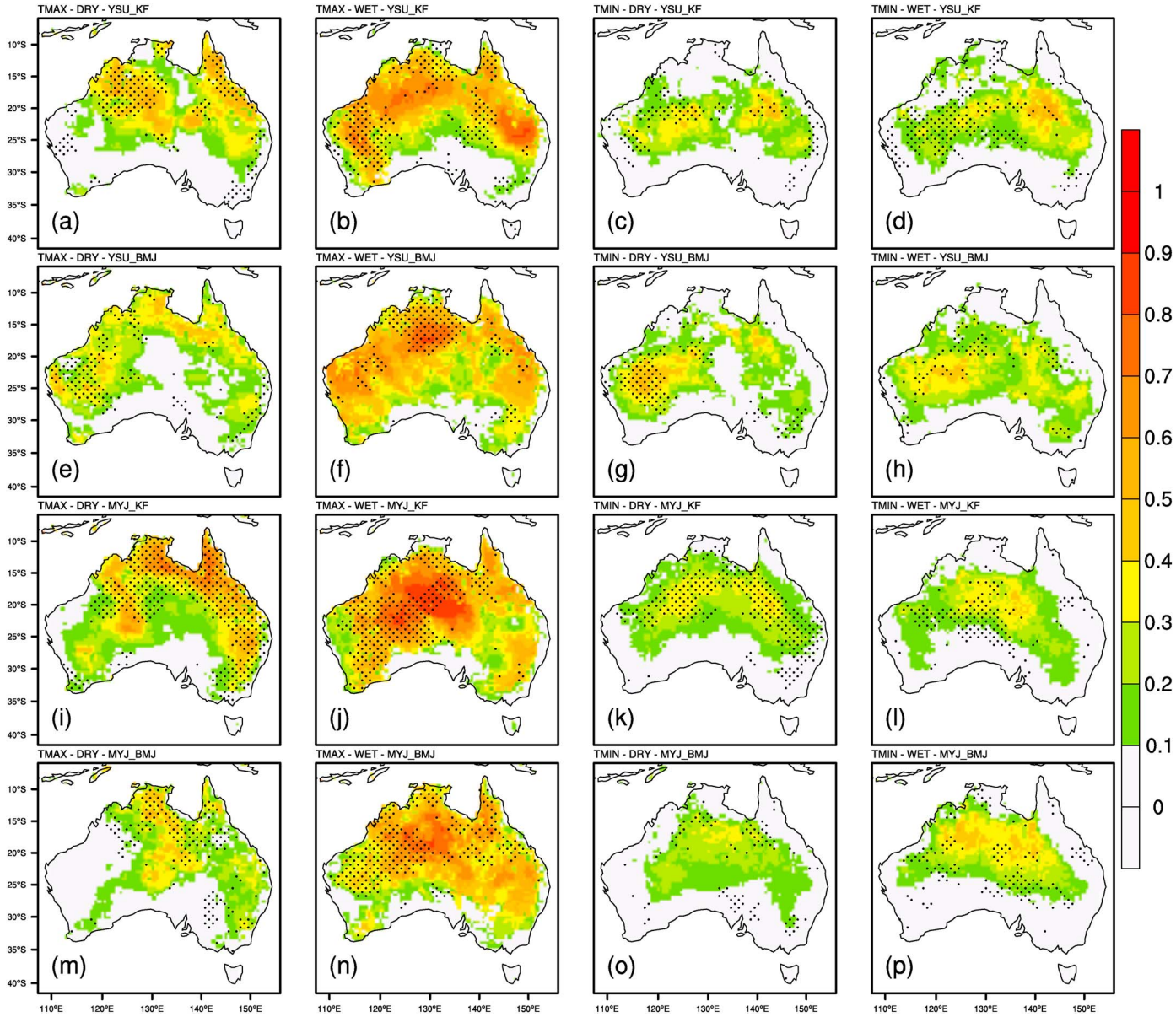

Figure 1. Soil moisture-temperature coupling strength ($\Delta\Omega$) for WRF-LIS-CABLE for the different configurations. (a–d) For YSU PBL with KF cumulus scheme, (e–h) for YSU PBL with BMJ cumulus scheme, (i–l) for MYJ PBL with KF cumulus scheme, and (m–p) for MYJ PBL with BMJ cumulus scheme. T_{MAX} $\Delta\Omega$ for the dry soil moisture case (Figures 1a, 1e, 1i, and 1m), T_{MAX} $\Delta\Omega$ for the wet soil moisture case (Figures 1b, 1f, 1j, and 1n), T_{MIN} $\Delta\Omega$ for the dry soil moisture case (Figures 1c, 1g, 1k, and 1o), and T_{MIN} $\Delta\Omega$ for the wet soil moisture case (Figures 1d, 1h, 1l, and 1p). Regions that are statistically significant at the 90% level are stippled.

September-October-November. For each physics configuration, the wet and dry soil moisture cases for the coupled ensemble simulations differ only by forcing data, whereas for the uncoupled ensemble simulations, the prescribed soil moisture states are selected from different ensemble members.

For the assessment of the soil moisture-atmosphere coupling strength, we use the $\Delta\Omega$ diagnostic employed in the GLACE-1 experiment. The definition of $\Delta\Omega$, the method for calculating statistical significance and further details on the experimental design can be found in the supporting information.

3. Results

We focus our analysis on the impacts of soil moisture on maximum (T_{MAX}) and minimum (T_{MIN}) 2 m air temperature. Figure 1 shows $\Delta\Omega$ for each combination of PBL, cumulus scheme, and soil moisture state for T_{MAX} and T_{MIN} (for mean temperature, T_{MEAN}, results see Figure S1).

Overall, the results for T_{MAX} (Figures 1a, 1b, 1e, 1f, 1i, 1j, 1m, and 1n) reveal strong soil moisture-temperature coupling during daytime, with $\Delta\Omega$ values of similar magnitude as those found for the GLACE-1 boreal summer "hot spots" [*Koster et al.*, 2006, Figure 8]. Results for all physics configurations suggest that the background climate is important for the diagnosed coupling strengths, with stronger $\Delta\Omega$ values diagnosed for wetter versus drier conditions (0.7–0.9 versus 0.2–0.7, compare Figures 1b, 1f, 1j, and 1n and Figures 1a, 1e, 1i, and 1m). The boundary layer and convection scheme have a weaker effect on the derived coupling strengths, although some nonnegligible differences exist for the dry year (Figures 1a, 1e, 1i, and 1m). For T_{MAX}, $\Delta\Omega$ is therefore more sensitive to interannual variability in meteorological drivers than the choice of PBL or cumulus convection scheme.

Contrary to the results for T_{MAX}, soil moisture-T_{MIN} coupling (Figures 1c, 1d, 1g, 1h, 1k, 1i, 1o, and 1p) shows smaller differences between the prescribed soil moisture cases, PBL scheme, cumulus scheme or the combination of PBL and cumulus schemes. In all model configurations, the T_{MIN} coupling strength values (0.1–0.5) over central Australia demonstrate that soil moisture still influences T_{MIN}, but nearer the coast the impact of soil moisture weakens. Overall, T_{MIN} coupling strength estimates appear robust to the modifications examined here, including whether soil moisture is in an El Niño-like or La Niña-like state.

We note that our results for soil moisture-precipitation coupling strength (Figure S2) show that $\Delta\Omega$ is small and not statistically significant. The magnitudes are comparable to GLACE-1 [*Koster et al.*, 2006, Figure 5] but less coherent, a consequence of the finer-scale resolution. For this reason, we focus on temperature effects in the present analyses.

4. Discussion

To examine the different T_{MAX} coupling strengths between the physics configurations for the dry soil moisture case (Figures 1a, 1e, 1i, and 1m) we explored the distribution of coupling strengths for a given soil moisture temporal mean and temporal variance prescribed in the uncoupled ensemble. The difference between all the configurations is the prescribed soil moisture in the uncoupled ensemble and it is from this forcing that we expect to see the clearest signal to explain the differences. The mean T_{MAX} coupling strength as a function of the prescribed soil moisture state is shown in Figure 2. The average T_{MAX} coupling strength decreases with mean soil moisture in both soil moisture cases (Figures 2a and 2b, derived from Figure S3) indicating that the transition from dry to wet soils influences T_{MAX} coupling through changes in the surface energy balance. Note that average T_{MAX} coupling strengths in Figure 2a and 2b are only indicative and do not fully reflect the distribution of coupling strengths shown in Figure 1.

Soil moisture influences both the energy and water balances through its impact on evapotranspiration [*Seneviratne et al.*, 2010]. Wetter soils lead to more energy partitioned into latent heat with less available for sensible heat. However, beyond a critical soil moisture threshold the rate of evaporation is no longer constrained by moisture availability, rather by energy availability. Conversely for drier soils, the moisture limitation on evaporation means more energy is available for sensible heating leading to an increase in surface temperatures. Therefore, the soil moisture limitation on evaporation can lead to a direct impact on T_{MAX} with saturated soils moving toward an energy limited evaporation regime with large-scale atmospheric dynamics imparting greater influence on surface temperatures.

For mean T_{MAX} coupling strength as a function of the soil moisture temporal variance (Figures 2c and 2d, derived from Figure S4), regions with high soil moisture variability are strongly coupled. This is a coherent feature irrespective of the WRF physics configuration. Further, beyond a critical soil moisture temporal variance, the mean T_{MAX} coupling strength remains constant with increasing variance, and this limit occurs at the same point in all WRF physics configurations. High soil moisture variability can lead to high variability in the latent and sensible heat fluxes, a result similar to *Guo et al.* [2006] who found that models with high evaporation variability tend to have higher coupling strength. From Figure 2, the critical component driving this variability is how soil moisture and associated surface fluxes are represented in the LSM, rather than how these fluxes affect the atmospheric component of the model.

The MYJ-KF physics combination is statistically significantly different from the other combinations in Figures 2a, 2c, and 2d at the 95% level and had the highest coupling strength for T_{MAX} dry soil moisture case (Figure 1i). This is reflected in Figure 2 for both the soil moisture temporal mean (Figure 2a) and variance (Figure 2c). The MYJ-KF configuration for the wet soil moisture case also has, on average, higher coupling

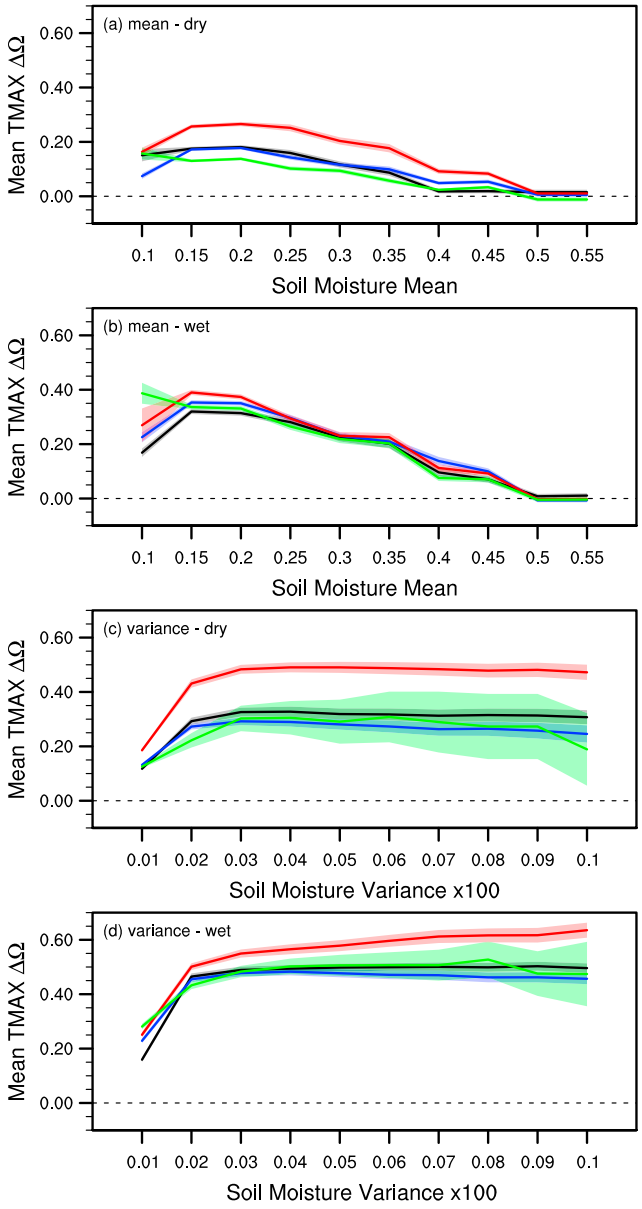

Figure 2. Mean T_{MAX} coupling strength ($\Delta\Omega$) as a function of the following: (a–b) temporal mean of soil moisture prescribed in the uncoupled ensembles for the dry and wet cases, (c–d) temporal variance of soil moisture prescribed in the uncoupled ensembles for the dry and wet cases. The lines show YSU–KF (black), YSU–BMJ (blue), MYJ–KF (red), and MYJ–BMJ (green) physics configurations. The full distributions of coupling strength around the mean values are shown in Figures S3 and S4. Shaded regions indicate the corresponding 95% confidence intervals for each physics configuration. The percentage of the domain for each soil moisture bin used to construct each PDF is shown in Figure S5.

strength consistently across the soil moisture variances in the uncoupled ensemble (Figure 2d). Clearly, specific combinations of the PBL and cumulus schemes have higher sensitivity to a given soil moisture variability. The differences displayed in Figure 2 were not associated with changes in the sample sizes for each soil moisture mean and variance (Figure S5).

A similar analysis for soil moisture-T_{MIN} coupling shows coupling is mostly insensitive to the prescribed soil moisture temporal mean with similar responses between the WRF physics configurations (Figures S6). This is as expected as T_{MIN} is modulated by net longwave emission and the ground heat flux rather than soil moisture-turbulent energy fluxes directly. However, the soil moisture-T_{MIN} coupling as a function of the prescribed soil moisture variance is sensitive at a 95% confidence level to the choice of PBL scheme in the wet soil moisture case (Figure S7). This reflects the difference in the surface layer scheme used for each

PBL scheme that is responsible for the development of a stable nocturnal boundary layer which in turn can influence T_{MIN}.

Contrasting the GLACE-like coupling strength between T_{MAX} and T_{MIN} has previously not been reported and our results show that the coupling strength differs strongly between T_{MAX} and T_{MIN} to reflect the different processes that influence daytime and nighttime temperatures. Daytime temperatures are the result of surface heating, entrainment, and growth of the PBL defined by the partitioning of available energy by soil moisture. Nighttime temperatures are modulated by cloud cover, net longwave emission and wind speed with minimal effects from soil moisture. T_{MIN} coupling is relatively insensitive to the prescribed soil moisture, or the combination of the PBL and convective cumulus schemes. T_{MAX} coupling, in contrast, is sensitive to the soil moisture state. This has implications for the original GLACE results [*Koster et al.*, 2006] which considered a single summer. Our results also suggest a strong dependency in the estimation of T_{MAX} coupling strength due to the choice of PBL and cumulus scheme, particularly in drier years. Further investigation into the reasons why some PBL-cumulus scheme combinations are more sensitive to soil moisture variance than others is clearly required.

5. Conclusions

We have implemented the GLACE-1 methodology in WRF and conducted simulations using different PBLs, cumulus convection schemes and soil moisture states to obtain a range of coupling strengths within a single model system for the Australian summer climate. Our results reveal a strong impact of soil moisture on T_{MAX} and T_{MEAN}, with coupling strengths for T_{MEAN} of similar magnitude to those reported for GLACE-1's boreal summer "hot spots". Our results demonstrate that coupling strength differs between T_{MAX} and T_{MIN}, associated with the different coupling mechanisms between the surface and the atmosphere. We find that the T_{MIN} coupling strength is largely insensitive to the soil moisture state and the choice of PBL and cumulus convection schemes. In contrast the T_{MAX} coupling strength is dependent on the soil moisture variability that is prescribed in the uncoupled simulations, and this dependency varies with the choice of PBL and cumulus convection scheme. For precipitation, the overall soil moisture-atmosphere coupling strength is not statistically significant in the El Niño and La Niña years investigated.

We conclude that for Australia, estimates of coupling strength for T_{MIN} are broadly robust to choice of year, PBL or cumulus convection scheme. In contrast, estimates of T_{MAX} coupling strength are dependent on the choice of year and on the choice of PBL or cumulus convection scheme. To determine which coupling strength is most realistic requires observations similar to those used by *Santanello et al.* [2009]. These are lacking over Australia and we are therefore limited to highlighting the sensitivity of $\Delta\Omega$ rather than determining which combination of physics in WRF provides the best coupling strength. Despite this limitation, our results highlight that estimates of coupling strength for T_{MAX} require a multimodel, multiseason, and multiyear experimental design [e.g., *Seneviratne et al.*, 2013], and the consideration of background climate and parameterization choices for soil moisture-atmosphere feedback.

Acknowledgments

This study was supported by the Australian Research Council Centre of Excellence for Climate System Science grant CE110001028. The computational modeling was supported by the NCI National Facility at the ANU, Australia. Annette L. Hirsch was supported by an Australian postgraduate award and CSIRO OCE postgraduate top up scholarship. The authors would like to thank two anonymous reviewers for their constructive feedback on this paper.

The Editor thanks two anonymous reviewers for their assistance in evaluating this paper.

References

Dee, D. P., et al. (2011), The ERA–Interim reanalysis: Configuration and performance of the data assimilation system, *Q. J. R. Meteor. Soc.*, *47*, 553–597, doi:10.1002/qj.828.

Evans, J. P., M. Ekström, and F. Ji (2012), Evaluating the performance of a WRF physics ensemble over South-East Australia, *Clim. Dyn.*, *39*, 1241–1258, doi:10.1007/s00382–011–1244–5.

Guo, Z., and P. A. Dirmeyer (2013), Interannual variability of land–atmosphere coupling strength, *J. Hydrometeor.*, *14*, 1636–1646, doi:10.1175/JHM–D–12–0171.1.

Guo, Z., et al. (2006), GLACE: The Global Land–Atmosphere Coupling experiment. Part II: Analysis, *J. Hydrometeor.*, *7*, 611–625, doi:10.1175/JHM511.1.

Hirsch, A. L., J. Kala, A. J. Pitman, C. Carouge, J. P. Evans, V. Haverd, and D. Mocko (2014), Impact of land surface initialization approach on sub–seasonal forecast skill: A regional analysis in the Southern Hemisphere, *J. Hydrometeor.*, *15*, 300–319, doi:10.1175/JHM–D–13–05.1.

Jaeger, E. B., and S. I. Seneviratne (2011), Impact of soil moisture–atmosphere coupling on European climate extremes and trends in a regional climate model, *Clim. Dynam.*, *36*, 1919–1939, doi:10.1007/s00382–010–0780–8.

Koster, R. D., et al. (2004), Regions of strong coupling between soil moisture and precipitation, *Science*, *305*, 1138–1140, doi:10.1126/science.1100217.

Koster, R. D., et al. (2006), GLACE: The Global Land–Atmosphere Coupling Experiment. Part I: Overview, *J. Hydrometeor.*, *7*, 590–610, doi:10.1175/JHM510.1.

Koster, R. D., et al. (2010), The contribution of land initialization to subseasonal forecast skill: First results from the GLACE–2 Project, *Geophys. Res. Lett*, *37*, L02402, doi:10.1029/2009GL041677.

Kumar, S. V., et al. (2006), Land Information System: An inter-operable framework for high resolution land surface modeling, *Environ. Model. Soft.*, *21*, 1402–1415, doi:10.1016/j.envsoft.2005.07.004.

Mei, R., G. Wang, and H. Gu (2013), Summer land–atmosphere coupling strength over the U.S.: Results from the Regional Climate Model RegCM4–CLM3.5, *J. Hydrometeor.*, *14*, 946–962, doi:10.1175/JHM–D–12–043.1.

Mueller, B., and S. I. Seneviratne (2012), Hot days induced by precipitation deficits at the global scale, *Proc. Natl. Acad. Sci.*, *109*, 12,398–12,403, doi:10.1073/pnas.1204330109.

Risbey, J. S., M. J. Pook, P. C. McIntosh, M. C. Wheeler, and H. H. Hendon (2009), On the remote drivers of rainfall variability in Australia, *Mon. Weather Rev.*, *137*, 3233–3253, doi:10.1175/2009MWR2861.1.

Santanello, J. A., C. D. Peters-Lidard, S. V. Kumar, C. Alonge, and W.-K. Tao (2009), A modeling and observational framework for diagnosing local land–atmosphere coupling on diurnal time scales, *J. Hydrometeor.*, *10*, 577–599, doi:10.1175/2009JHM1066.1.

Seneviratne, S. I., et al. (2013), Impact of soil moisture-climate feedbacks on CMIP5 projections: First results from the GLACE–CMIP5 experiment, *Geophys. Res. Lett.*, *40*, 5212–5217, doi:10.1002/grl.50956.

Seneviratne, S. I., T. Corti, E. L. Davin, M. Hirschi, E. B. Jaeger, I. Lehner, B. Orlowsky, and A. J. Teuling (2010), Investigating soil moisture–climate interactions in a changing climate: A review, *Earth Sci. Rev.*, *99*, 125–161, doi:10.1016/j.earscirev.2010.02.004.

Skamarock, W. C., J. B. Klemp, J. Dudhia, D. O. Gill, D. M. Barker, M. G. Duda, X.-Y. Huang, W. Wang, and J. G. Powers, (2008), A description of the Advanced Research WRF Version 3, *NCAR Tech. Report, Note NCAR/TN–475+STR*, National Center for Atmospheric Research, Boulder, Colo.

Wang, Y. P., E. Kowalczyk, R. Leuning, G. Abramowitz, M. R. Raupach, B. Pak, E. van Gorsel, and A. Luhar (2011), Diagnosing errors in a land surface model (CABLE) in the time and frequency domains, *J. Geophys. Res.*, *116*, G01034, doi:10.1029/2010JG001385.

Wei, J., and P. A. Dirmeyer (2010), Toward understanding the large–scale land–atmosphere coupling in the models: Roles of different processes, *Geophys. Res. Lett.*, *37*, L19707, doi:10.1029/2010GL044769.